Title

AN INVESTIGATION OF THE STATES OP 2s, ld SHELL NUCLEI BASED ON THE FOUR-PARTICLE, FOUR-HOLE STATE IN 16O

Authors

Tewari, S.N.
Struble, G.L.

Publication Date

1969-09-01

Submitted to Physical Review

UCRL-18985
Preprint

Cy 2

AN INVESTIGATION OF THE STATES OF 2s, 1d SHELL NUCLEI BASED ON THE FOUR-PARTICLE, FOUR-HOLE STATE IN ^{16}O

S. N. Tewari and G. L. Struble

September 1969

AEC Contract No. W-7405-eng-48

LAWRENCE RADIATION LABORATORY
UNIVERSITY of CALIFORNIA BERKELEY

UCRL-18985
Cy 2

DISCLAIMER

AN INVESTIGATION OF THE STATES OF 2s,1d SHELL NUCLEI BASED ON THE FOUR-PARTICLE, FOUR-HOLE STATE IN ^{16}O*

S. N. Tewari

Lawrence Radiation Laboratory
University of California
Berkeley, California 94720

and

G. L. Struble

Lawrence Radiation Laboratory and
Department of Chemistry,
University of California
Berkeley, California 94720

September 1969

ABSTRACT

The four-particle, four-hole state in ^{16}O and the corresponding states in the even-even, N = Z nuclei of the 2s,1d shell have been investigated in the framework of the Hartree-Fock approximation. Detail calculations were performed in each case to determine the most stable Hartree-Fock solution. By assuming a simple model the excitation energies of the band heads were calculated which showed that ^{24}Mg is the last nucleus where a state analogous to the four-particle, four-hole state in ^{16}O might be observed. Energy levels have been calculated in ^{16}O, ^{20}Ne and ^{24}Mg using a basis of good angular momentum states. A comparison between the predicted and the obeserved energy spectrum has been shown. In ^{16}O, calculations have been performed both with phenomenological and realistic interactions and the results have been compared. The accuracy of the projected angular momentum states from the twelve-particle, four-hole solution in ^{24}Mg has been estimated and shows that the projected states in this case are close to the eigenstates. We have demonstrated that one of two 0^+ states observed around 7 MeV in ^{20}Ne is a eight-particle, four-hole state.

INTRODUCTION

The analysis of the experimental results of Carter et al.[1] suggests that many of the low-lying positive parity excited states in ^{16}O may be approximately fitted into rotational bands. This identification is further supported by large E2-transitions encountered,[2,3] e.g.

$$B(E2, 2_1^+ \rightarrow 0_2^+) = 40\ e^2f^4$$

and

$$B(E2, 4_1^+ \rightarrow 2_1^+) = 117 \pm 10\ e^2f^4 \quad .$$

Although the rotational features in ^{16}O are not as striking as in the case of heavy deformed nuclei of the rare-earth region, the interpretation of its experimental data in terms of a rotating deformed intrinsic state is very tempting.

During the last decade the Hartree-Fock (HF) method has been successfully applied to calculate intrinsic states of the deformed nuclei in the 2s,1d shell.[4] The application of this method to calcualte intrinsic states in ^{16}O therefore seems desirable. A number of HF calculations has already been performed[5,6] in ^{16}O and an analysis of the results of these calculations leads to the important conclusion that the intrinsic state of the rotational band starting at 6.05 MeV is mainly composed of a four-particle, four-hole (4p-4h) state.

By using certain symmetries of the HF density Banerjee et al.[6] have shown that the most stable shape of the 4p-4h intrinsic state is ellipsoidal

(triaxial). They have also calculated the energy levels of the band by a crude approximation and their results are encouraging for undertaking a more rigorous calculation in the basis of good angular momentum states projected out from the triaxial 4p-4h state. We have performed such a calculation and our results, to be presented in the text, are in good agreement with the experiment. However, in order to obtain a better agreement with the experiment and in particular to account for the observed electromagnetic transition rates it is essential that the 4p-4h state, the closed p shell and the two-particle, two-hole (2p-2h) states be admixed. In fact, the observed electron-position pair transition of the excited 0^+ to the ground state can be explained through such admixtures only.[7,8] The shell-model calculations of Brown and Green,[9] and those of Celenza, et al.[10] estimate such admixtures to the extent of 13% to 16%. Since their predicted B(E2)'s are in satisfactory agreement with a number of observed B(E2)'s, their calculations may be taken as an excellent verification of the HF results concerning the importance of the 4p-4h state.

It may be pointed out here that the investigation by Krieger[11] shows that the 4p-4h state can not be brought down below 20 MeV above the ground state by HF calculations with present generation of realistic forces. However, despite this unpleasant feature, the 4p-4h state calculated with realistic potentials may be physically quite important. Energy levels calculated from this intrinsic state may compare well with the energy levels observed within the rotational band starting at 6.05 MeV. A detailed discussion on this aspect will be presented elsewhere in the text.

The fact of the 4p-4h state playing the major role in generating the intrinsic state of the lowest rotational band in ^{16}O makes it very tempting to examine if similar n-particle 4-hole (np-4h) states exist in the even-even, N = Z nuclei (4n nuclei) of the 2s,1d shell. (The notation np-4h will refer to the states in 4n nuclei constructed by promoting four particles from the closed p shell to the 2s,1d shell. For example, in ^{20}Ne it will refer to the 8p-4h state.) An analysis of the results of the various calculations[12-14] performed using the basis of 2s,1d shell for the excited states of ^{20}Ne lends strong support to this hypothesis. There are two 0^+ states in ^{20}Ne observed around 7 MeV, whereas all these calculations predict only one 0^+ state in this region. The other 0^+ states predicted by these calculations are nowhere close to 7 MeV. In particular, the failure of the complete shell-model calculation[14] in predicting two 0^+ states around 7 MeV convincingly demonstrates that the basis of 2s,1d shell is not adequate. Therefore one of the 0^+ states is most likely due to the multiple particle-hole excitations from the ^{16}O core. The 4p-4h structure of second 0^+ state in ^{16}O which lies at approximately the same energy suggests that one of the 0^+ states in ^{20}Ne around 7 MeV may be a 8p-4h state.

There is no such evidence for the existence of np-4h states in other 4n nuclei of the 2s,1d shell. However our preliminary calculations reported earlier[15] show that such a state may be important in ^{24}Mg. In ^{28}Si, ^{32}S and ^{36}Ar it is very doubtful that such states will be of any relative importance because the $1d^{5/2}$ shell is completely filled in this region.

We have performed HF calculations for the np-4h states in all the 4n nuclei of the 2s,1d shell. In ^{20}Ne and ^{24}Mg where np-4h HF states are found

to lie at reasonable energies relative to their ground states, energy levels have been calculated by projecting out good angular momentum states. The accuracy of the projected states have been tested in ^{24}Mg. In other interesting cases like ^{16}O and ^{20}Ne similar accuracy tests are extremely involved because the shape of their intrinsic states is triaxial. In Sections II, and III we will describe the methods of our calculations. Section IV contains the numerical results and discussions. A summary is presented in Section V.

SECTION II

As mentioned in the introduction, the concept of an intrinsic state plays a very important role in describing the rotational bands of deformed nuclei. It represents, in an internally correlated manner, all the members of the band; and the physical quantities characterizing the band, such as the moments of inertia etc., can all be derived from a knowledge of the intrinsic state. By assuming that it can be represented by a Slater determinant, a definite procedure for obtaining the intrinsic wave function is provided by the HF theory. Excellent discussions on the HF method are available in literature[4,16] and only an outline of the method will be presented here.

A. HF Equations

Let α, β, etc., represent a complete set of single-particle basis states for which a_α^+, a_α are, respectively, the creation and destruction operators with respect to some reference vacuum $|0\rangle$. In the second-quantized form, the nuclear Hamiltonian is written as

$$H = \sum_{\alpha,\beta} \langle \alpha|K|\beta \rangle \; a_\alpha^+ a_\beta + \frac{1}{4} \sum_{\alpha,\beta,\gamma,\delta} \langle \alpha\beta|V|\delta\gamma \rangle_{AS} \; a_\alpha^+ a_\beta^+ a_\gamma a_\delta \qquad (1)$$

where K is the one-body kinetic energy operator and V is the two-body interaction operator.

Given the Hamiltonian defined in Eq. (1) the prescription of the HF theory for determining the intrinsic wave function Φ of a nucleus with A nucleons out of the vacuum $|0\rangle$ consists in finding a unitary transformation U which defines a new basis of single-particle states $|\lambda\rangle$ and the associated creation and destruction operators b_λ^+, b_λ:

$$b_\lambda^+ = \sum_\alpha u_\alpha^\lambda a_\alpha^+$$

$$b_\lambda = \sum_\alpha u_\alpha^{\lambda *} a_\alpha \qquad (2)$$

such that Φ defined as the Slater determinant:

$$|\Phi\rangle = \prod_{\lambda=1}^{A} b_\lambda^+ |0\rangle \qquad (3)$$

is a solution of the stationary condition:

$$\frac{\delta}{\delta U} \langle \Phi | H | \Phi \rangle = 0 \quad . \qquad (4)$$

The condition (4) is satisfied if the HF matrix

$$h_{\alpha\beta} = \langle \alpha | K | \beta \rangle + \sum_{\lambda=1}^{A} \langle \alpha\lambda | V | \beta\lambda \rangle_{AS} \qquad (5)$$

is just diagonal on the new basis, i.e. if

$$h|\lambda\rangle = e^\lambda |\lambda\rangle \quad . \qquad (6)$$

The Eqs. (5) and (6) define a self-consistency problem because the HF Hamiltonian h is defined in terms of the new orbitals $|\lambda\rangle$. The solution to this problem is obtained through an iterative procedure:

a. An initial set of orbitals $|\lambda\rangle$, A in number, are guessed.

b. HF Hamiltonian h is constructed using Eq. (5) and diagonalized.

c. Finally A appropriate eigenvectors of h give a new set of orbitals $|\lambda\rangle$ which are again used to perform the operation b. This process is repeated until successive diagonalizations produce the same set of orbitals $|\lambda\rangle$.

B. Symmetries of HF Hamiltonian

The definition of the HF Hamiltonian h as given by Eq. (5) does not imply that h be invariant under the symmetry operations which keep the actual Hamiltonian H invariant. To see this point more clearly let us introduce the one-body density operator ρ:

$$\rho = \sum_{\lambda} a_{\lambda}^{+} a_{\lambda} \quad . \tag{7}$$

In terms of the density operator ρ, the HF Hamiltonian h can be written as

$$h_1 = K_1 + \mathrm{Tr}_2 V_{12} \rho_2 \tag{8}$$

where the subscripts refer to the particles in whose space the operators operate. Since the density operator ρ as defined in Eq. (7) does not necessarily possess the symmetries of H, therefore it is also true that h does not necessarily possess the symmetries of H. However, it is clear from Eq. (8) that whatever symmetries of H are incorporated into density ρ, they also become incorporated in the HF Hamiltonian h.

The importance of the various symmetries of the actual Hamiltonian in relation to the HF Hamiltonian has been studied in great detail by many authors.[6,17,18] Banerjee *et al.*[6] have

recently shown that the general exchange nature and the short range of the effective shell-model Hamiltonian lead to the existence of symmetries of HF density ρ of $4n$ nuclei under the following operations:

(1) Time reversal; T,

(2) reflection through a plane, e.g. the x-z plane; $Pe^{-i\pi J_y}$, and

(3) rotation by π about an axis in the plane of the reflection symmetry, e.g. the z axis; $e^{i\pi J_z}$,

where P in (2) is the parity operator. They further argue that as an implication of this one should not expect parity mixing in the HF wave fucntions of these nuclei. The calculation of Bassichis, Kerman, and Svenne[18] strongly support this implication because they find no advantage in parity mixing unless the tensor force is increased to nearly twice its normal strength. Similar conclusions about parity admixture are also reached by Pal and Stamp[17] in their HF calculations with the Yale potential.

Besides the symmetries (1), (2), and (3) the HF density of $4n$ nuclei also has approximate symmetry under rotations in spin-isospin space. A discussed by Banerjee et al.,[6] this symmetry is once again due to the exchange nature of the effective interaction because it leads to the occupation of each space orbital four times.

The knowledge of the symmetries of HF density is of great importance in carrying out the HF calculations. It simplifies the choice of the initial ρ in the iterative program required in the HF calculations. Clearly, a completely arbitrary choice for the initial ρ can immensely increase the labor in such calculations.

SECTION III

A. Angular Momentum Projection

The calculation of the intrinsic wave function, though very useful, is certainly not enough by itself to provide quantitative description of the rotational band. One has to project out states of good angular momentum from the intrinsic wave function in order to calculate the physical quantities, viz., energies of the rotational levels, electromagnetic moments etc. An alternative to the angular momentum projection could be used for the calculation of energy levels by making use of the moment of inertia which can be directly computed from the intrinsic single-particle wave functions and energies. However due to the ambiguities involved in the calculations of moment of inertia,[19,20] the alternate approach is not very reliable. Given the intrinsic wave function the method of angular momentum projection is certainly more reliable and accurate. There are several methods[21] for projecting out angular momentum states and in our calculations we have applied the method based on the use of the Hill-Wheeler integral.[22] In the following we will briefly describe this method with reference to the calculation of energy levels.

Let M and K denote the projection of J along the laboratory and body-fixed z axis respectively. The angular momentum projection operator P^J_{MK} is given by

$$P^J_{MK} = \frac{2J+1}{8\pi^2} \int d\Omega \; D^J_{MK}(\Omega) \; R(\Omega) \tag{9}$$

Where $R(\Omega)$ is the rotation operator:

$$R(\Omega) = e^{-i\alpha J_z} e^{-i\beta J_y} e^{-\gamma J_z} \tag{10}$$

in which Ω stands as an abbreviation for the Euler angles α, β, γ, and the matrix elements of which are

$$D^J_{MK}(\Omega) = \langle JM|R(\Omega)|JK\rangle \quad . \tag{11}$$

The integral $\int d\Omega$ is an abbreviation for the triple integral:

$$\int d\Omega = \int_0^{2\pi} \int_0^{\pi} \int_0^{2\pi} d\alpha \sin\beta \, d\beta \, d\gamma \quad . \tag{12}$$

The operator P^J_{MK} has the following properties:

$$\left(P^J_{MK}\right)^+ = P^J_{MK}$$

and (13)

$$P^J_{MK} P^J_{MK} = P^J_{MK} \quad .$$

To discuss the procedure for the calculation of energy levels let us consider the case when the intrinsic state Φ is triaxial. Acting on Φ the operator P^J_{MK} first projects out the angular momentum eigenstate,

$$\psi^J_{KK} = P^J_{KK}|\Phi\rangle \tag{14}$$

with quantum numbers J and K and then steps ψ^J_{KK} into a state ψ^J_{MK} with quantum numbers J and M. The projected states satisfy the following orthogonality

relations:

$$\langle \psi^J_{MK} | \psi^{J'}_{M'K'} \rangle = \delta_{JJ'} \, \delta_{MM'} \, X^J_{KK'} \tag{15}$$

where

$$X^J_{KK'} = \langle \Phi | P^J_{KK'} | \Phi \rangle \quad . \tag{16}$$

A state of good angular momentum Ψ^J_M corresponding to the intrinsic state Φ is now given by

$$\Psi^J_M = \sum_K \alpha^J_K \, \psi^J_{MK} \quad . \tag{17}$$

It is clear that the coefficients α^J_K do not depend on M. The energy of the state Ψ^J_M is determined from the variational principle

$$\delta \langle \Psi^J_M | H | \Psi^J_M \rangle / \delta \alpha^J_K = 0 \quad . \tag{18}$$

This is equivalent to diagonalizing H in the non-orthogonal basis spanned by the wave functions ψ^J_{MK}. Therefore the solution to Eq. (18) reduces to solving the following set of linear equations

$$\sum_K \left[Y^J_{MK} - E^J \, X^J_{MK} \right] \alpha^J_K = 0 \tag{19}$$

where

$$Y^J_{MK} = \langle \Phi | H P^J_{MK} | \Phi \rangle \tag{20}$$

and

$$X^J_{MK} = \langle \Phi | P^J_{MK} | \Phi \rangle \quad . \tag{21}$$

The quantities Y^J_{MK} and X^J_{MK} are 3-fold integrals of the functions $Y(\Omega)$ and $X(\Omega)$ respectively,

$$Y(\Omega) = \langle \Phi | HR(\Omega) | \Phi \rangle$$

and

$$X(\Omega) = \langle \Phi | R(\Omega) | \Phi \rangle \quad . \tag{22}$$

These functions, and the integrals Y^J_{MK} and X^J_{MK} can be evaluated by following the techniques discussed in Refs. 21 and 23.

The eigenvalues E^J and the eigenfunctions Ψ^J_M determined by solving the Eq. (19) in the space of the wave functions ψ^J_{MK} correspond to the approximate eigenvalues and the eigenfunctions of the actual Hamiltonian H.

In case when the intrinsic state Φ is axially symmetric, the projection operator P^J_{MK} defined by Eq. (9) reduces to

$$P^J_{KK} = \frac{2J+1}{2} \int_0^{\pi} d^J_{KK}(\beta)\, e^{-i\beta J_y} \sin\beta \, d\beta \tag{23}$$

where $d^J_{KK}(\beta)$ is the reduced rotation matrix,

$$d^J_{KK}(\beta) = \langle JK | e^{-i\beta J_y} | JK \rangle \quad . \tag{24}$$

The Eq. (17) reduces to an identity and consequently the Eq. (19) is reduced to

$$E^J = Y^J_{KK}/X^J_{KK}$$

$$= \frac{\langle \Phi_K | HP^J_{KK} | \Phi_K \rangle}{\langle \Phi_K | P^J_{KK} | \Phi_K \rangle} \quad . \tag{25}$$

The energy given by Eq. (25) can be more easily evaluated than in Eq. (19). Various simplfying features of this calculation are discussed in great detail in Ref. 24.

B. Accuracy of the Projected States

It is important to know how accurate are the projected states when compared to the actual eigenstates, i.e., the states which are obtained by the complete shell-model calculation. A simple accuracy test can be developed in the following way:

Let Ψ^J denote the projected angular momentum state. We have

$$H\Psi^J = E^J\Psi^J + \sum a_n \phi^J_n \tag{26}$$

where E^J is given by Eq. (19) in the triaxial case and by Eq. (25) in the axial case. The wave functions ϕ^J_n together with Ψ^J define a complete orthonormal basis. The coefficients a_n are given by

$$a_n = \langle \Phi^J_n | H | \Psi^J \rangle \quad . \tag{27}$$

where E_o' and ε_α' in Eq. (33) are respectively the experimental binding energy of ^{16}O and a set of single-particle energies relative to ^{16}O. The normal product in Eq. (33) refers to the ^{16}O core and to the ^{4}He core in Eq. (34). If we assume that the self-consistent orbitals in ^{4}He and ^{16}O are the same, then the primed and unprimed quantities are related by

$$E_o = E_o' - 4\varepsilon'_{1p_{1/2}} - 8\varepsilon'_{1p_{3/2}} + \frac{1}{2}\sum_{\beta\beta'} \langle \beta\beta' | V | \beta\beta' \rangle_{AS} \quad , \tag{35}$$

$$\varepsilon_\alpha = \varepsilon_\alpha' - \sum_{\beta} \langle \alpha\beta | V | \alpha\beta \rangle_{AS} \quad , \tag{36}$$

where the indices β,β' run over the 1p shell only.

In Table I we list the experimental energies ε_j' relative to ^{16}O and the equivalent energies ε_j relative to ^{4}He. The experimental binding energy increase between ^{4}He and ^{16}O is 99.3 MeV. Our calculated binding energy increase is 100.05 MeV. Even assuming an increase in the Coulomb repulsion of about 10 MeV, we obtain good agreement with the experimental number.

In the case of ^{16}O we performed an additional HF calculation using a realistic interaction which was defined by the effective matrix elements of the Yale potential calculated by Shakin et al.[25] Although the HF energy of the deformed 4p-4h intrinsic state of ^{16}O calculated from this interaction is expected to be very poor it may then contain important dynamical correlations to provide a good explanation for the nuclear properties within the band. Further discussion will be presented later in this section with the help of tables.

The HF calculations for the np-4h states can be very difficult in practice because there can exist many HF solutions with different or similar shapes. However, the work of the calculation can be considerably simplified if one knows the most stable shapes of the n particles in 2s,1d shell and 4 holes in 1p shell, i.e. ^{12}C.

Recently Banerjee et al.[6] have predicted the most stable shapes of the HF solutions of the 4n nuclei in 2s,1d shell from a consideration of short range attraction and general exchange properties of the effective two-nucleon interaction. Their predicted shapes are listed for the nuclei of interest in Table II. These shapes correspond to results known from earlier HF[4,21] and SU_3[26] calculations. Now this information and the fact that the most stable shape of ^{12}C has a spheroidal oblate density distribution allows one to predict the most stable shapes of the np-4h states, if we assume that the most stable np-4h state is that which gives the maximum overlap of the density distributions of the 2s,1d shell nucleons with the ^{12}C density distribution.[6] For example, consider the 4p-4h state in ^{16}O. The four particles in 2s,1d shell correspond to ^{20}Ne having a spheroidal prolate density distribution for the most stable state. This can be combined with the oblate spheroidal density of ^{12}C in various ways. It can be seen that the maximum density overlap will not be obtained by superimposing the two densities so that their resultant density is rotationally invariant about the z axis; a better overlap is obtained by rotating the ^{12}C density so that the two axes of rotational symmetry are perpendicular. The combined density destribution is thus triaxial. That this is true has already been verified in Ref. 6. Our HF calculations of the 4p-4h state of ^{16}O also

confirm the correctness of this result. Using analogous arguments for the remaining nuclei we predict their most stable shapes, i.e. their lowest intrinsic states as listed in Table III.

To verify the validity of these arguments other HF solutions were also calculated in these nuclei. The properties of the various solutions are listed in Table IV. Comparing Table III with Table IV it is seen that the lowest solution in each case is that expected from these arguments. We consider this as one of the important conclusions of our calculations.

In Fig. 1 are plotted the excitation energies E_x of the band heads of the np-4h states as a function of the mass number A. The quantities E_x were calculated by the following equation:

$$E_x = (E_G - A\langle J^2 \rangle) - (E_{ph} - A'\langle J^2 \rangle) \quad , \tag{37}$$

where E_G and A are respectively the HF energy and the moment of inertia parameter for the ground state, E_{ph} and A' are the corresponding quantities for the np-4h state. The parameters A and A' were calculated by the first order cranking model.[27]

The result on ^{16}O as shown in Fig. 1 is completely unsatisfactory because the band head of the 4p-4h state comes about 2 MeV below the ground state. This is due to the fact that the cranking model predicts too large a value for the parameter A'. Since the value A is zero for the spherical ground state no compensation occurs from the possible cancellation implied in Eq. (37).

The results for the 4n nuclei in the 2s,1d shell are physically quite significant. In this case where both A and A' contribute, and the excitation

energies E_x are perhaps not much affected by the errors in A and A'. The cancellation implied in Eq. (37) may minimize the effect of such errors. It is interesting to note from Fig. 1 that the excitation energy gradually increases through ^{24}Mg and then increases rapidly. This is quite understandable because $1d_{5/2}$ shell is expected to be completely filled around ^{28}Si and hence it is relatively more costly to promote four particles from the closed 1p shell to the 2s,1d shell. It is quite clear from the results that ^{24}Mg is the last nucleus where it might be possible to find a state which is dominantly np-4h state.

To understand properly the significance of the results in Fig. 1, the following limitations of our calculations should be noted. (i) The choice of the same set of single-particle energies ε_j for all the 4n nuclei, $16 \leqslant A \leqslant 36$, is not quite justified. However, this may not be a serious defect because it can be seen from the discussions of Ripka[4] on the extrapolation of ε_j through the 2s,1d shell that the variation of ε_j with A could be small. (ii) Further correction is expected due to not taking into account the center of mass (c.m.) excitation likely to be important for the np-4h states. An estimate of the c.m. excitation can be obtained by evaluating the quantity $S \equiv \langle \Phi | \underline{A}^+ \cdot \underline{A} | \Phi \rangle$ where the operator A was defined by Baranger and Lee.[28] The value of S for the triaxial 4p-4h state has been calculated by Giraud and Sauer[29] and found to be very small, S = 0.009. Therefore we expect that the c.m. excitation will not be important for the np-4h states of the remaining 4n nuclei. It should be pointed out that the condition $S \ll 1$ implies that the c.m. stays close to the external origin (to which the motion of the individual nucleons are referred), and therefore the presence

of phenomenological ϵ_j in the nuclear Hamiltonian H is justified. (iii) The calculation of the inertial parameter by the first order cranking model may be a poor approximation. Despite these limitations, we believe that the results in Fig. 1 are of considerable physical significance. A rigorous calculation for the energy levels of the np-4h intrinsic states in ^{16}O, ^{20}Ne and ^{24}Mg has been performed.

The energy levels have been calculated by using the techniques of angular momentum projection discussed in Section IIIA. The single particle wave-functions of the HF determinants used in the calculations are given in Tables V - VI. A comparison between the calculated and experimental energy levels are given in Fig. 2 and Table VII.

It can be seen from the Fig. 2 that the calculated and experimental energy levels are on the whole in good agreement up to about 5 MeV in ^{16}O. It may be noted that the 0^+ state of the 4p-4h band has been plotted at the zero of the energy scale in the figure. Our calculation predicts this 0^+ state at 3.06 MeV above the ground state as compared to the experimental value of 6.06 MeV. This is however a great improvement over the corresponding result in Fig. 1. By increasing the energy separations between the 1p and 2s,1d shell by about 1 MeV it should be possible to bring our predicted 0^+ state close to 6.06 MeV. Such an increment is unlikely to change the structure of the 4p-4h intrinsic state and hence the energy levels of the 4p-4h band will remain the same as shown in Fig. 2. Confining ourselves to the comparison within the band we note that the predicted and experimental 4^+ states are very close in energy. The close agreement lends strong support to the conjecture of Brown and Green[9] that the 4^+ state is purely a 4p-4h state. We further note that the perdicted 2^+ state is about 0.4 MeV above

the corresponding observed state. This is a gratifying feature. It is known that the 2p-2h states admix with the states of the 4p-4h band. Brown and Green[9] predicted approximately 14% and 5% of such admixtures for the 2^+ and 0^+ states of the 4p-4h band respectively. Therefore it is clear that as a result of such admixtures our calculated 2^+ state will be further lowered in energy to produce a better agreement with experiment. The corresponding effect on the 0^+ state of the 4p-4h band will be relatively smaller. The 3^+ state is predicted to be degenerate with the 4^+ state and about 1 MeV lower than the corresponding observed state. As we go to the higher members of the band the agreement with the experiment further deteriorates. It appears that the K = 2 band is not adequately represented in the triaxial HF state. We have calculated the energies[30] from the triaxial HF ground state in ^{24}Mg. The comparison of these energies with the experiment shown in Fig. 2 lends support to this conjecture. The 0^+ and 2^+ states predicted around 10 MeV and 11 MeV respectively in ^{24}Mg have been calculated from its 12p-4h HF state. It is significant to note that there also exists an experimental 0^+ state around 10 MeV in ^{24}Mg.

The results on ^{20}Ne are of considerable importance. It seems quite evident from them that one of the two 0^+ states observed around 7 MeV is mostly a 8p-4h state and the other is a β-vibrating state described by the Tamm-Dancoff approximation (T.D.A.). It can be further seen from Fig. 2 that our calculation also reproduces many of the excited states in ^{20}Ne. However, a one-to-one correspondence between the predicted and observed levels cannot be made without further theoretical and experimental studies. An interesting feature of the calculated spectrum is the presence of a 3^+

state at about 10.5 MeV. Our experience in ^{16}O and ^{24}Mg shows that the 3^+ state calculated from the triaxial HF solution is always about 1 MeV lower than the corresponding experimental state. Therefore a 3^+ state should be expected experimentally in ^{20}Ne at about 11.5 MeV.

It should be noted that the levels labelled by (TH) in ^{20}Ne are described by a linear combination of projected angular momentum states of two types. The first type is obtained from the HF ground state and the second type is obtained from an intrinsic state constructed out of the HF ground state by TDA. The wave functions of the first set of 0^+, 2^+, 4^+ and 6^+ levels are mostly of the first type and those of remaining (TH) levels are mostly of the second type. The mixing between the two types of states is J-dependent and varies from 2% to 4%. Details on this calculation can be found in an earlier publication by one of us.[12]

The accuracy of the projected angular momentum states has been tested for the 12p-4h HF solution in ^{24}Mg by the method discussed in Section III B. The results are listed in Table VIII. It is clear from the numbers in column 4 that the projected states in this case are, to a very good approximation, the actual eigenstates of the Hamiltonian. In view of this conclusion it follows that the admixtures of the 10p-2h and ground states with the 12p-4h state in ^{24}Mg are negligible.

It has been pointed out earlier in this section that the first order cranking model predicts a large value for the moment of inertia (m.i.) parameter A' of the 4p-4h band in ^{16}O. The values of $A(A_x, A_y, A_z)$ for the various intrinsic states of the different 4n nuclei are given in Table IV. It will be instructive to calculate the energies of the 4p-4h band by the Davydov-Filipov (DF) model[31] using the predicted values of $A'(A'_x, A'_y, A'_z)$

compare the energies thus obtained with the energies obtained by the projection method. Such a comparison is presented in Table IX. A similar comparison is also presented in the same table for the 8p-4h state of ^{20}Ne. It is clear from the Table IX that the m.i. parameter A' from the cranking model is quite large in ^{16}O, about twice its value obtained from the projection method. In the case of ^{20}Ne both the methods predict about the same value for A'. It should be noted that it is only some average value of the m.i. parameter which can be inferred from the Table IX.

We will now conclude the discussions with some remarks on the significance of the results of HF calculations with the realistic forces for the 4p-4h state in ^{16}O. Our HF calculation with the Yale potential yields, as expected, a triaxial shape for the most stable 4p-4h intrinsic state. The HF energy of the intrinsic state is 37.62 MeV relative to the spherical ground state. The energies of the various J states of the intrinsic state have also been calculated by using the projection techniques discussed in Sec. IIIA. The $J = 0^+$ member of the intrinsic state comes down in energy by 5.80 MeV after projection to give it a net excitation energy of 31.82 MeV.

Krieger has recently made a detail study of the 4p-4h state by using a velocity-dependent potential which was especially derived to be used in the HF calculation. The energy of the 4p-4h intrinsic state is predicted in his calculations as 26.1 MeV relative to the ground state. Assuming an expected gain of 6 MeV after projection the excitation energy of the 0^+ state comes to approximately 20 MeV. This value is certainly very large when compared to the experimental value of 6.06 MeV. In view of the various refinements considered by Krieger in his calculations it may be stated that the HF calculations with realistic forces cannot reproduce the experimental 0^+ state at 6.06 MeV.

The failure of the HF calculations with realistic forces in reproducing the 0^+ state at 6.06 MeV is not surprising. It is well known from the various publications[17,25,32] that the HF and the Brueckner-Hartree-Fock (BHF) calculations underbind all the nuclei to a large extent and do not reporduce the experimental single-particle energies at all well. The results of Pal and Stamp[17] obtained from the Yale potential for the ground state of ^{16}O show that the energy gap between the $1p_{1/2}$ and $1d/_{5/2}$ orbitals is about 4.3 MeV larger than that obtained from experiment. Thus it is expected that the $J = 0^+$ member of the 4p-4h intrinsic state will have a much higher excitation energy compared to 6.06 MeV. Nevertheless it is our contention that the 4p-4h intrinsic state obtained from the realistic forces is physically important and it contains the necessary dynamical correlations to explain the properties of the different member states of the 4p-4h band. That this is a justifiable contention is strongly suggested by the HF calculations with Yale potential on ^{20}Ne. Although the binding energy of ^{20}Ne is poorly reproduced, the energy spectrum of the ground band is very well reproduced. The example of ^{20}Ne clearly suggests to expect a similar agreement in the case of the 4p-4h intrinsic state of ^{16}O. In Table X is presented a comparison of the energy levels from the 4p-4h intrinsic states calculated with the Yale potential and the phenomenological potential defined in Eq. (32). It is quite clear from the Table X that our contention is physically meaningful and justified.

SECTION V

Summary

We have shown that the projected angular momentum states from the triaxial HF determinant of the 4p-4h state in ^{16}O provides a good quantitative interpretation of the energy spectrum of the rotational band starting at 6.06 MeV. By assuming a reasonable phenomenological interaction in the HF calculation it is also possible to reproduce the 0^+ state at 6.06 MeV. This is no more true if a realistic interaction is used in the HF calculation.

Our calculation on ^{20}Ne shows that one of the two 0^+ states around 7 MeV in ^{20}Ne is a 8p-4h state and the other can be obtained from the deformed ground state by the TDA. In ^{24}Mg we have predicted a 0^+ state at 10.31 MeV. The existence of an experimental 0^+ state at about the same energy in ^{24}Mg suggests that the experimental studies on its structure will be extremely interesting. It is clear from our calculations that ^{24}Mg is the last nucleus where a state corresponding to the four-particle excitation from the ^{16}O core might be observed.

ACKNOWLEDGMENTS

We are indebted to Dr. M. K. Banerjee, Dr. A. Goodman, Dr. P. Sauer, and Dr. B. Giraud for useful discussions. We especially are grateful to Dr. Giraud for making his projection code available to us. We would also like to thank Mr. P. S. Rajasekker for help in programming.

FOOTNOTES AND REFERENCES

* Work performed under the auspices of the U. S. Atomic Energy Commission.

1. E. B. Carter, G. E. Mitchell, and R. H. Davis, Phys. Rev. 133B, 1421, 1434 (1964).
2. S. Gorodetzky, P. Mennrath, W. Benenson, P. Chevallier, and F. Scheibling, J. Phys. 24, 887 (1963).
3. J. D. Larson and R. H. Spear, Nucl. Phys. 56, 497 (1964).
4. G. Ripka, Advan. Phys. 1, 183 (1968) and all references mentioned therin.
5. W. H. Bassichis and G. Ripka, Phys. Letters 15, 320 (1965).
6. G. J. Stephenson Jr. and M. K. Banerjee, Phys. Letters 24B, 209 (1966); M. K. Banerjee, C. A. Levinson, and G. J. Stephenson Jr., Phys. Rev. 178, 1709 (1969).
7. E. Boeker, Phys. Letters 21, 69 (1966).
8. G. F. Bertsch, Phys. Letters 21, 70 (1966).
9. G. E. Brown and A. M. Green, Nucl. Phys. 75, 401 (1966).
10. L. S. Celenza, R. M. Dreizler, A. Klein, and G. J. Dreiss, Phys. Letters 23, 241 (1966).
11. S. J. Krieger, Phys. Rev. Letters 22, 97 (1969).
12. S. N. Tewari, Phys. Letters 29B, 5 (1969). (Energies calculated in this paper have small errors. Corrected results are given in the present paper.)
13. W. H. Bassichis, C. A. Levinson, and I. Kelson, Phys. Rev. 136B, 380 (1964).
14. E. C. Halbert, Y. E. Kim, T. T. S. Kuo, and J. B. McGrory, International Nuclear Physics Conference, Gatlinburg, Tennessee, 1966 (Academic Press Inc., New York, 1967) p. 531.
15. G. L. Struble and S. N. Tewari, Proceedings of the International Nuclear Physics Conference, Montreal, Canada, 1969.

16. M. Baranger, 1962 Cargése Lectures in Theoretical Physics (W. A. Benjamin, Inc., New York, 1963).

17. M. K. Pal and A. P. Stamp, Phys. Rev. 158, 924 (1967);
A. P. Stamp, Nucl. Phys. A105, 627 (1967).

18. W. H. Bassichis, A. K. Kerman, and J. P. Svenne, International Conference on Nuclear Physics, Gatlinburg, Tennessee, 1966 (Academic Press Inc., New York, 1967) p. 855.

19. I. Kelson, Phys. Rev. 160, 775 (1967).

20. M. K. Banerjee, D. d'Oliveira, and G. J. Stephenson Jr., Moment of Inertia in Hatree-Fock Theory, to be published.

21. G. Ripka, Lectures in Theoretical Physics (University of Colorado Press, Boulder, Colorado, 1966).

22. D. L. Hill and J. A. Wheeler, Phys. Rev. 89, 1106 (1953).

23. B. Giraud, Proc. of Summer School on Nuclear Physics in Herceg Novi, Yugoslavia, August 1966.

24. S. N. Tewari and D. Grillot, Phys. Rev. 177, 1717 (1969).

25. C. M. Shakin, Y. R. Waghmare, and M. H. Hull Jr., Phys. Rev. 161, 1006 (1967).
C. M. Shakin, Y. R. Waghmare, M. Tomaselli, and M. H. Hull Jr., Phys. Rev. 161, 1015 (1967).

26. M. Harvey, Advan Phys. 1, 67 (1968).

27. D. R. Inglis, Phys. Rev. 96, 1059 (1954).

28. E. Baranger and C. W. Lee, Nucl. Phys. 22, 157 (1961).

29. B. Giraud and P. U. Sauer, Parity-Mixed Hartree-Fock Solutions in the 2s-1d Shell, to be published.

30. B. Giraud and P. U. Sauer, Proceedings of the International Nuclear Physics Conference, Montreal, Canada, 1969.

31. A. S. Davydov and G. F. Filipov, Nucl. Phys. 8, 237 (1958).

32. K. T. R. Davies, M. Baranger, R. M. Tarbutton, and T. T. S. Kuo, Phys. Rev. 177, 1519 (1969).

TABLE CAPTIONS

Table I. Single particle energies used in the calculations with the Rosenfeld force. The energies in the second column are relative to a ^{16}O core and energies in the third column are relative to a ^{4}He core.

Table II. Shapes of the most stable ground intrinsic states of the N = Z even-even nuclei in the s-d shell as predicted by HF calculations.

Table III. Predicted shapes of the most stable np-4h solutions of the HF equations for N = Z even-even nuclei in the s-d shell.

Table IV. Properties of HF intrinsic states for N = Z even-even nuclei in the s-d shell. Columns 1, 2, and 3 list the nucleus, its particle hole nature, and the expectation value of the Hamiltonian. Columns 4 and 5 describe the shape of the nucleus by presenting the expectation value for the operations $r^2Y_0^2$ and $r^2(Y_2^2 + Y_{-2}^2)$ respectively. Columns 6, 7, and 8 give the inertial parameters $A_i = \hbar^2/2\mathcal{I}_i$ where $\mathcal{I}_i$ is the i^{th} component of the moment of inertia. Columns 9, 10, and 11 present the expectation values of the operators J_i^2 in units of $\hbar^2$ where J_i is the i^{th} component of the total angular momentum. Finally in column 12 we give the position of the band head by subtracting the rotational energy from the intrinsic states energy. All energy units are in MeV and all solutions were calculated with a Rosenfeld force and experimental single particle energies.

Table V. Single particle energies in MeV, and wave functions for the 4p-4h HF solutions for ^{16}O. The first solution was obtained using a Rosenfeld force and experimental single particle energies. The second solution was obtained with effective matrix elements of the Yale potential.

Table VI. Single particle energies in MeV and the wave functions for the 8p-4h HF solution in ^{20}Ne and the 12p-4h HF solution in ^{24}Mg. These solutions were obtained using a Rosenfeld force and experimental single particle energies.

Table VII. A tabulation of the experimental and theoretical energies presented in Fig. 2. For convenience of comparison some of the theoretical energies have been ommitted. The labels (ph) and (TH) are discussed in the text and Fig. 2.

Table VIII. A tabulation of the results from a calculation of the energy fluctuation for the states of good angular momentum projected from the intrinsic 12p-4h HF state for ^{24}Mg given in Table VI. Since the ratios in column 4 are nearly unity, the projected solutions are a good approximation to the exact eigenstates of the Hamiltonian.

Table IX. A comparison of excitation energies relative to the band head for states of good angular momentum obtained from HF intrinsic states by exact angular momentum projection and using the Davydov-Filipov model. The HF solutions for ^{20}Ne and ^{24}Mg are given in Table VI.

Table X. A comparison of excitation energies relative to the band head for states of good angular momentum obtained by exact projection from HF intrinsic states given in Table V. Column 2 lists the energies obtained with the Rosenfeld force and column 3 gives the energies obtained with the Yale potential. The good agreement suggests that the intrinsic states are very similar.

Table I.

Spherical harmonic oscillator states	Single-particle energies	
j	ε_j'(MeV)	ε_j(MeV)
$1p_{3/2}$	-21.83	1.06
$1p_{1/2}$	-15.67	7.22
$1d_{5/2}$	- 4.14	8.26
$2s_{1/2}$	- 3.27	1.97
$1d_{3/2}$	0.94	13.34

Table II.

Nucleus	Shape
^{20}Ne	Prolate Axial
^{24}Mg	Triaxial
^{28}Si	Oblate Axial
^{32}S	Triaxial
^{36}Ar	Oblate Axial

Table III.

Nucleus	Hole-particle Structure	Shape
^{16}O	4p-4h	triaxial
^{20}Ne	8p-4h	triaxial
^{24}Mg	12p-4h	oblate axial
^{28}Si	16p-4h	triaxial
^{32}S	20p-4h	oblate axial
^{36}Ar	24p-4h	oblate axial

Table IV.

Nucleus	Type	$\langle H \rangle$	$\langle r^2 Y_0^2 \rangle$	$\langle r^2 y_2^2 \rangle$	A_x	A_y	A_z	$\langle J_x^2 \rangle$	$\langle J_y^2 \rangle$	$\langle J_z^2 \rangle$	$\langle H-AJ^2 \rangle$
^{16}O	0p 0h	-99.98	0.	0.	∞	∞	∞	0.	0.	0.	-99.98
^{16}O	4p 4h	-91.37	17.62	-4.14	0.3669	0.4193	0.9494	7.722	9.814	3.803	-101.93
^{16}O	4p 4h	-83.57	17.28	0.	0.3434	0.3434	∞	8.050	8.050	0.	-89.10
^{16}O	4p 4h	-87.38	-11.38	0.	0.8227	0.8227	∞	4.412	4.412	0.	-94.62
^{20}Ne	4p 0h	-139.25	14.36	0.	0.3658	0.3658	∞	7.725	7.725	0.	-144.90
^{20}Ne	8p 4h	-129.62	19.41	-9.34	0.2302	0.3376	0.5044	11.61	13.05	7.923	-140.69
^{20}Ne	8p 4h	-105.62	20.27	0.	0.4063	0.4063	∞	12.91	12.91	0.	-116.11
^{20}Ne	8p 4h	-116.81	-21.40	0.	0.2914	0.2914	∞	11.88	11.88	0.	-123.73
^{24}Mg	8p 0h	-182.75	16.26	-5.04	0.2284	0.2683	0.5767	11.51	11.17	4.45	-190.94
^{24}Mg	12p 4h	-173.17	-28.43	0.	0.3030	0.3030	∞	14.40	14.40	0.	-181.90
^{24}Mg	12p 4h	-148.67	23.04	0.	0.1677	0.1677	∞	16.91	16.91	0.	-154.34
^{28}Si	12p 0h	-231.70	-21.30	0.	0.2434	0.2434	∞	11.84	11.84	0.	-237.46
^{28}Si	16p 4h	-202.56	-24.11	-4.05	0.2065	0.3615	0.5857	18.57	11.14	4.10	-212.82
^{32}S	16p 0h	-283.36	-16.47	-4.14	0.2044	0.2796	0.5146	14.21	9.56	4.72	-291.37
^{32}S	20p 4h	-238.74	-19.81	0.	0.1680	0.1680	∞	13.94	13.94	0.	-241.08
^{36}A	20p 0h	-340.65	-13.13	0.	0.2848	0.2848	∞	9.49	9.49	0.	-346.06
^{36}A	24p 4h	-270.77	-6.78	0.	0.2309	0.2309	∞	3.59	3.59	0.	-272.43

Table V.

HF single-particle energy (MeV)	Basis states									
	$1s_{1/2}^{1/2}$	$1p_{3/2}^{-3/2}$	$1p_{3/2}^{1/2}$	$1p_{1/2}^{1/2}$	$1d_{5/2}^{-3/2}$	$1d_{5/2}^{1/2}$	$1d_{5/2}^{5/2}$	$2s_{1/2}^{1/2}$	$1d_{3/2}^{-3/2}$	$1d_{3/2}^{1/2}$
					Rosenfeld Potential					
-24.195		0.16470	0.92411	-0.34480						
-17.973		0.78576	0.08837	0.61219						
-15.158					0.05061	0.66086	0.06734	-0.63632	-0.03906	-0.38697
-4.364					0.71092	0.47876	0.15173	0.42292	0.09952	0.23151
-3.773		0.59620	-0.37176	-0.71157						
-2.201					0.48838	-0.32237	-0.41335	-0.54905	0.29375	0.31459
0.858					0.45226	-0.46238	0.36765	0.00219	-0.02272	-0.66781
2.343					0.12381	0.08410	-0.80572	0.27747	-0.29275	-0.40709
6.323					0.18344	-0.09628	0.13125	-0.19440	-0.90336	0.29325

(continued)

Table V (continued)

HF single-particle energy (MeV)	$1s_{1/2}^{1/2}$	$1p_{3/2}^{-3/2}$	$1p_{3/2}^{1/2}$	$1p_{1/2}^{1/2}$	$1d_{5/2}^{-3/2}$	$1d_{5/2}^{1/2}$	$1d_{5/2}^{5/2}$	$2s_{1/2}^{1/2}$	$1d_{3/2}^{-3/2}$	$1d_{3/2}^{1/2}$
					Basis states					
					Yale Potential					
-43.597	0.98291				0.02115	0.08009	0.04772	0.13106	-0.05083	-0.07069
-23.253		-0.02215	0.86612	-0.49935						
-17.331		-0.77852	0.29842	0.55214						
-7.127	0.00469				-0.03270	0.67904	-0.05084	-0.61611	0.05406	-0.39080
-7.064		0.62723	0.40098	0.66768						
-0.570	0.03048				0.80339	-0.37565	0.08926	-0.24666	0.21437	-0.31265
1.689	0.09409				-0.17778	-0.29607	0.54430	-0.61048	-0.27759	0.35479
4.410	0.00804				-0.46649	-0.49150	-0.13578	-0.07667	-0.16567	-0.69927
7.048	0.07355				0.17128	-0.11590	-0.75377	-0.28196	-0.48610	0.26049
9.972	0.13646				-0.27292	-0.22072	-0.32296	-0.29039	0.77957	0.24862

Table VI.

HF single-particle energy	Basis states								
	$1p_{3/2}^{-3/2}$	$1p_{3/2}^{1/2}$	$1p_{1/2}^{1/2}$	$1d_{5/2}^{-3/2}$	$1d_{5/2}^{1/2}$	$1d_{5/2}^{5/2}$	$2s_{1/2}^{1/2}$	$1d_{3/2}^{-3/2}$	$1d_{3/2}^{1/2}$
				^{20}Ne					
-28.736	0.20316	0.92476	-0.32177						
-23.201	0.75474	0.06146	0.65314						
-17.627				0.20650	0.64651	-0.06139	-0.70447	0.13543	-0.14489
-15.169				0.67767	0.25620	0.05127	0.35818	0.21434	0.54613
-4.876				0.11103	-0.55791	-0.51236	-0.45114	0.29279	0.35303
-4.833	0.62378	-0.37555	-0.68547						
-0.880				0.65813	-0.38378	0.17236	-0.04616	0.00043	-0.62269
0.669				0.14139	0.20755	-0.81299	0.27428	-0.38797	-0.22411
5.022				0.18073	-0.12145	0.20105	-0.30748	-0.83634	0.34373

(continued)

Table VI (continued)

HF single-particle energy	Basis states								
	$1p_{3/2}^{-3/2}$	$1p_{3/2}^{1/2}$	$1p_{1/2}^{1/2}$	$1d_{3/2}^{-3/2}$	$1d_{5/2}^{1/2}$	$1d_{5/2}^{5/2}$	$2s_{1/2}^{1/2}$	$1d_{3/2}^{-3/2}$	$1d_{3/2}^{1/2}$
					^{24}Mg				
-32.923	1.0								
-29.162		0.66679	0.74525						
-19.458					0.39790		0.88151		-0.25418
-19.006						1.0			
-15.238				0.56742				-0.82343	
-5.991		0.74525	-0.66679						
-2.238				0.82343				0.56742	
-1.418					0.84706		-0.24659		0.47083
3.882					0.35237		-0.40265		-0.84481

UCRL-18985

Table VII.

J	^{16}O Experiment (MeV)	^{16}O Theory (MeV)	J	^{20}Ne Experiment (MeV)	^{20}Ne Theory (MeV)	J	^{24}Mg Experiment (MeV)	^{24}Mg Theory (MeV)
0^+	0.0	0.0	0^+	0.0	0.0	0^+	0.0	0.0
0^+	6.06	3.06	2^+	1.63	1.20(TH)	2^+	1.37	1.40
2^+	6.92	4.34	4^+	4.25	3.80(TH)	4^+	4.12	2.58
2^+	9.85	5.87	0^+	6.72	5.76(TH)	2^+	4.23	2.60
4^+	10.36	7.13	0^+	7.20	6.79(ph)	3^+	5.23	3.95
3^+	11.08	7.05	2^+	7.43	8.05(ph)	4^+	6.00	3.96
0^+	11.26		2^+	7.84	8.61(TH)	0^+	6.44	
2^+	11.53		6^+	8.79	7.81(TH)	2^+	7.35	
4^+	13.89	8.54	4^+	9.16	9.19(ph)	6^+	8.12	7.27
			2^+	9.50	9.31(ph)	4^+	8.44	7.55
			3^+		10.48(ph)	5^+	8.86	8.96
			4^+	11.07	10.66(ph),10.97(TH)	6^+	9.52	8.82
						0^+	10.68	10.31(ph)
						2^+	11.99	11.44(ph)

Table VIII.

J	$\langle J\|H\|J\rangle^2$ $(MeV)^2$	$\langle J\|H^2\|J\rangle$ $(MeV)^2$	$\frac{E}{C} = \frac{\langle J\|H\|J\rangle}{\langle J\|H^2\|J\rangle^{1/2}}$
0	31469.2344	31475.9764	0.9999
2	31070.0905	31106.8366	0.9994
4	30162.4846	30265.1558	0.9983
6	28799.9567	28996.9486	0.9966

Table IX.

J	^{16}O Projection (MeV)	^{16}O DF Model (MeV)	^{20}Ne Projection (MeV)	^{20}Ne DF Model (MeV)
0^+	0.	0.	0.	0.
2^+	1.28	2.35	1.26	1.66
2^+	2.81	4.59	2.52	2.62
3^+	3.99	6.94	3.69	4.29
4^+	4.07	7.81	2.40	5.27
4^+	5.48	10.14	3.87	6.94
4^+	10.30	16.77	5.71	9.24

Table X.

J	Phenomenological force (MeV)	Realistic force (MeV)
0^+	0.0	0.0
2^+	1.28	1.23
2^+	2.81	2.31
3^+	3.99	3.50
4^+	4.07	3.87
4^+	5.48	5.25
4^+	10.30	9.48

FIGURE CAPTIONS

Fig. 1. Excitation energies of np-4h intrinsic states in the N = Z even-even nuclei of the s-d shell. The excitation energies are computed using Eq. 37 in the text.

Fig. 2. A comparison of experimental and calculated energies in ^{16}O, ^{20}Ne, and ^{24}Mg. The zero of energy in ^{16}O has been taken at the first excited 0^+ state. For ^{20}Ne and ^{24}Mg the zero of energy corresponds to the ground state. In ^{20}Ne, $J^+(ph)$ corresponds to the projected state from the 8p-4h intrinsic state while $J^+(TH)$ is a linear combination of projected states from the HF and TDA intrinsic states.

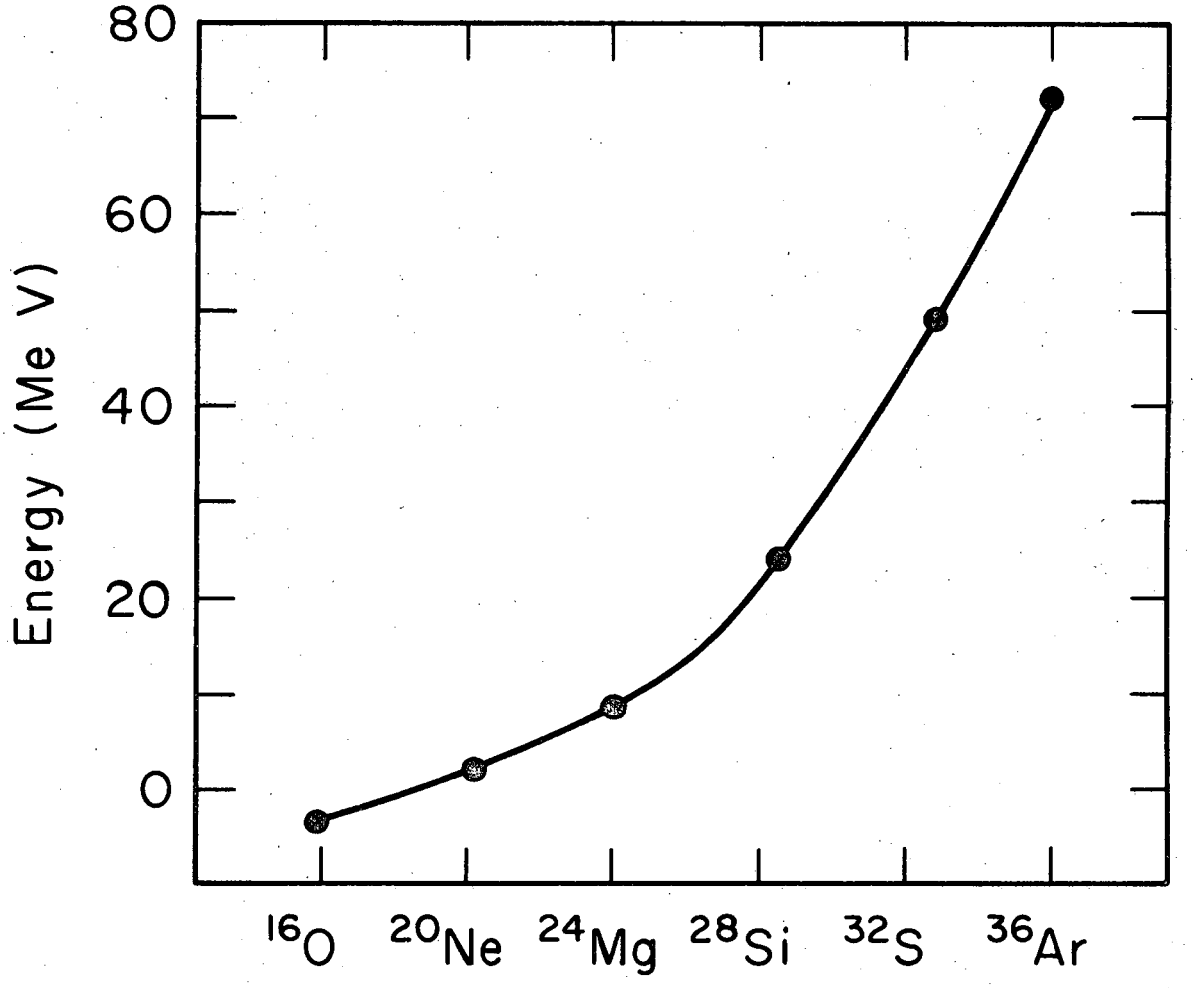

XBL699-3783

Fig. 1

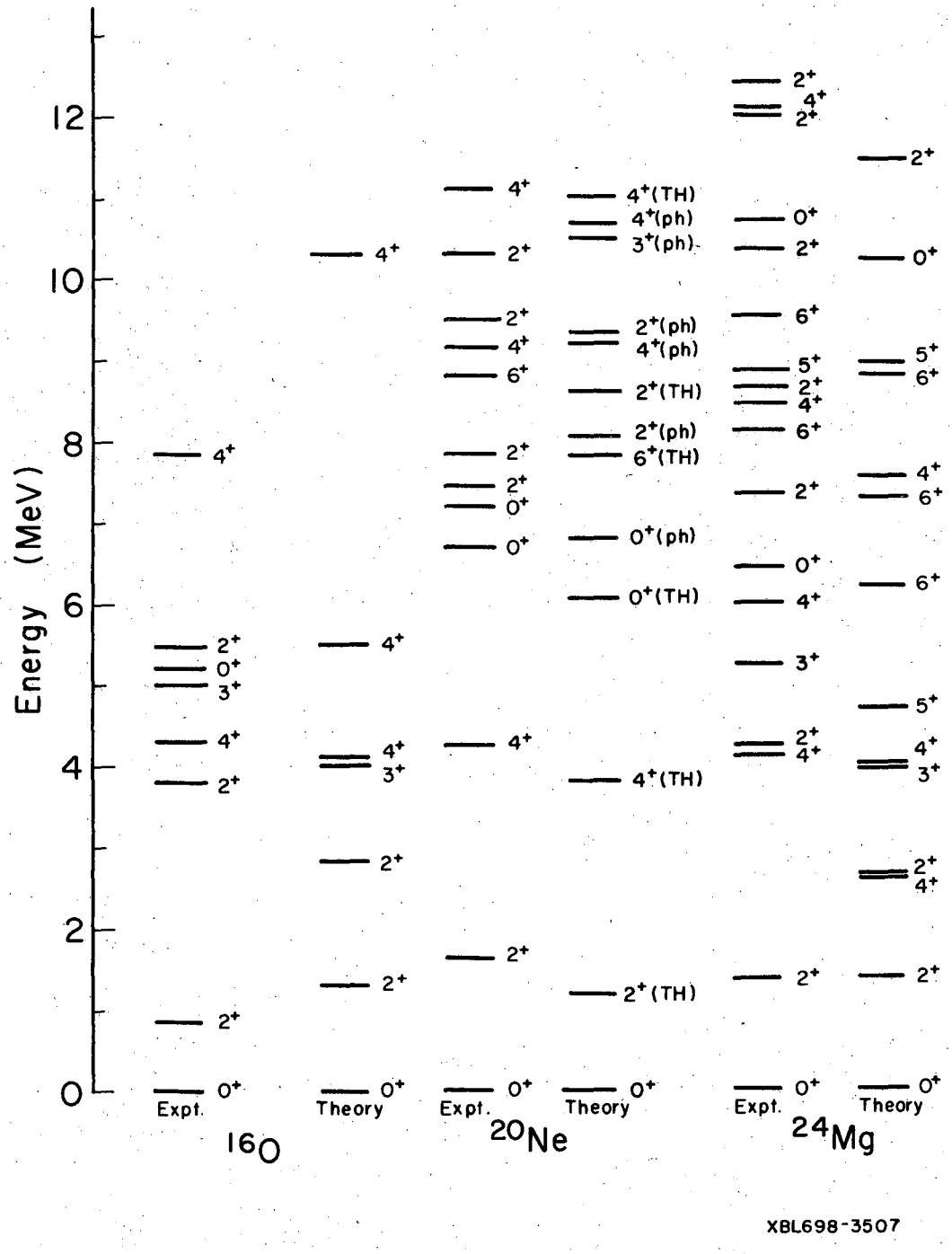
Energy (MeV)
0
2
4
6
8
10
12
Expt.
Theory
Expt.
Theory
Expt.
Theory
16O
20Ne
24Mg
0+
2+
4+
3+
6+
5+
4+(TH)
4+(ph)
3+(ph)
2+(ph)
4+(ph)
2+(TH)
6+(TH)
0+(ph)
0+(TH)
XBL698-3507

Fig. 2

TECHNICAL INFORMATION DIVISION
LAWRENCE RADIATION LABORATORY
UNIVERSITY OF CALIFORNIA
BERKELEY, CALIFORNIA 94720